CrossMark

Research Article

Repositioning of Anti-parasitic Drugs in Cyclodextrin Inclusion Complexes for Treatment of Triple-Negative Breast Cancer

Josefina Priotti,[1] **María Virginia Baglioni,**[2] **Agustina García,**[3] **María José Rico,**[2] **Darío Leonardi,**[1,3] **María Celina Lamas,**[1,3,5] **and Mauricio Menacho Márquez**[2,4]

Abstract. Drug repositioning refers to the identification of new therapeutic indications for drugs already approved. Albendazole and ricobendazole have been used as anti-parasitic drugs for many years; their therapeutic action is based on the inhibition of microtubule formation. Therefore, the study of their properties as antitumor compounds and the design of an appropriate formulation for cancer therapy is an interesting issue to investigate. The selected compounds are poorly soluble in water, and consequently, they have low and erratic bioavailability. In order to improve their biopharmaceutics properties, several formulations employing cyclodextrin inclusion complexes were developed. To carefully evaluate the *in vitro* and *in vivo* antitumor activity of these drugs and their complexes, several studies were performed on a breast cancer cell line (4T1) and BALB/c mice. *In vitro* studies showed that albendazole presented improved antitumor activity compared with ricobendazole. Furthermore, albendazole:citrate-β-cyclodextrin complex decreased significantly 4T1 cell growth both in *in vitro* and *in vivo* experiments. Thus, new formulations for anti-parasitic drugs could help to reposition them for new therapeutic indications, offering safer and more effective treatments by using a well-known drug.

KEY WORDS: albendazole; repositioning; breast cancer cell line; cyclodextrin.

INTRODUCTION

Cancer is a major cause of mortality worldwide despite of the large number of treatment and prevention studies. According to the World Health Organization estimates, by 2030, the global incidence is expected to increase to 21.7 million cancer cases [1–3]. Currently, chemotherapy is one of the most effective strategies to avoid the proliferation of malignant tumors [3, 4]. However, the ability of cancer cells to become resistant to different drugs remains a significant impediment to successful chemotherapy [1]. In this sense, drug repositioning has emerged as an alternative strategy for cancer treatment. Drug repositioning refers to the identification of new therapeutic indications for drugs already approved [5, 6]. There are innumerable advantages as well as challenges for drug repositioning. For instance, drug repositioning is an alternative strategy to accelerate drug discovery, since the discovery of new active pharmaceutical ingredients takes a lot of effort and economic impact [7–9]. Moreover, repositioned drugs are relatively inexpensive and carry minimal risk due to the availability of previous pharmacological, safety, and toxicology data, significantly decreasing the costs for treatments with associated low toxicity [10–14]. Drug repositioning, as a new strategy, benefits patients by offering safer and effective treatments using well-known drugs [15, 16].

Albendazole (ABZ) and ricobendazole (RBZ) are benzimidazole derivatives usually employed as antihelmintic compounds [17, 18]. The pharmacological activities of these drugs are focused in the inhibition of tubulin polymerization and blockage of glucose uptake. Thus, these compounds produce depletion of glycogen stores and decrease the adenosine triphosphate (ATP) formation in the larval and adult stages of parasites [19–21]. Microtubule formation is involved in cell division; therefore, its inhibition is currently one of the goals of medicinal chemistry in cancer chemotherapy [22].

Research on ABZ antitumor activity has been carried out on ovarian cancer cell lines [23, 24], and other studies

Josefina Priotti and María Virginia Baglioni contributed equally to this work.

[1] IQUIR-CONICET, Suipacha 570, 2000, Rosario, Argentina.
[2] Instituto de Genética Experimental, Facultad de Ciencias Médicas, UNR, 2000, Rosario, Santa Fe, Argentina.
[3] Departamento de Farmacia, Facultad de Ciencias Bioquímicas y Farmacéuticas, UNR, Suipacha 570, 2000, Rosario, Argentina.
[4] Instituto de Investigaciones para el Descubrimiento de Fármacos de Rosario (IIDEFAR, UNR-CONICET), UNR, Ocampo y Esmeralda, 2000, Rosario, Argentina.
[5] To whom correspondence should be addressed. (e–mail: mlamas@fbioyf.unr.edu.ar)

aaps

were performed on HCT-116 (a colorectal cancer cell line) in which ABZ was formulated as hydroxypropyl-β-cyclodextrin (HP-β-CD) inclusion complexes [25, 26].

Castro *et al.* (2016) reported an interesting study on MCF7 breast cancer cells, showing that ABZ promotes oxidative DNA damage, which induces DNA fragmentation, apoptosis, and cell death [1]. In addition, Sorlie *et al.* (2003) described the effect of ABZ on MCF7, an estrogen receptor-positive cell line, extending the putative use of ABZ for the treatment of triple-negative breast tumors, the type of breast cancer with worse associated prognosis and limited therapeutic options [27, 28].

Despite their therapeutic efficacy, both ABZ and RBZ present poor aqueous solubility and limited absorption after oral administration. Pharmaceutical technology has developed several strategies to overcome solubility and absorption limitations of insoluble drugs such as solid dispersions [29], micellar formulations [30, 31], nano- and microstructured systems [20, 32, 33], co-crystals [34], and cyclodextrin (CD) inclusion complexes [35–39].

CDs are cyclic oligosaccharides, formed by glucopyranose units linked by covalent bonds α-1,4 forming a torus-like macroring shape, having an inner cavity with hydrophobic affinity and an outer surface with hydrophilic affinity [40, 41]. The locations of hydrophobic molecules inside the CD cavity usually produce significant improvement in many attributes, such as solubility, bioavailability, and stability [42].

β-CD has reached pharmaceutical relevance despite its low aqueous solubility, since chemical modifications increase this parameter due to the loss of the crystalline solid state. Furthermore, Lajos Szente and Jozsef Szejtli [43] postulated that the random substitution of any hydroxyl group produces an interference of the stable hydrogen bond system around the β-CD rims causing an enhancement of the aqueous solubility. Thus, many CDs have been synthesized to enhance the physicochemical properties of poorly soluble drugs, such as methyl-β-CD, HP-β-CD, sulfobutyl ether-β-CD, succinyl-β-CD, and citrate-β-CD [35–37, 39, 42, 44, 45]. Several techniques have been proposed for the preparation of CD inclusion complexes, which can be grouped into three categories: methods in solid state, methods in semi-solid state, or methods in solution. This latest involves removing the solvent from solutions of drug and CD by coevaporation/coprecipitation, spray-drying, or colyophilization [46]. Spray-drying involves feeding an aqueous solution into an atomizer that produces small droplets which are exposed to relatively high air temperatures in a short time [47]. In the present work, the spray-drying technique was selected because it strongly influences the properties of the obtained material such as size, morphology, and shape that generally increase dissolution rate [48]. Thus, the use of CDs as pharmaceutical excipients is an excellent practice to improve the physicochemical and pharmaceutical properties of poorly soluble drugs [42].

Therefore, the goal of this work was to prepare ABZ and RBZ-CD inclusion complexes by spray-drying procedure to study their putative use for triple-negative breast cancer treatment. These promising CD formulations could help to reposition ABZ and RBZ for new therapeutic indications offering safer and effective treatments employing well-known drugs.

MATERIALS AND METHODS

Materials

ABZ was obtained from Parafarm (Buenos Aires, Argentina). RBZ was kindly donated by Laboratorio Proagro SA (Rosario, Argentina). β-CD was donated by Roquette. S-β-CD and C-β-CD were synthesized in our laboratory as described previously [36, 37]. 4T1 cells were kindly provided by Dr. N. Zwirner (IBYME-CONICET), RPMI 1640 was purchased from Gibco (Waltham, Massachusetts, USA), and WST-1 (2-(4-Iodophenyl)-3-(4-nitrophenyl)-5-(2,4-disulfophenyl)-2H-tetrazolium) reagent was from Sigma-Aldrich (St. Louis, MO, USA). All other chemicals were of analytical grade.

Methods

Phase Solubility Diagrams

The stoichiometry and equilibrium constants for complex formation were determined by phase-solubility studies. Water solutions of β-CD and their derivatives were prepared using increasing concentrations from 0 to 50 mM. After that, an excess amount of each active pharmaceutical ingredient (API) was added. These solutions were kept in sealed vials, under stirring at 180 rpm for 72 h at room temperature. Solutions were filtered through a 0.45-μm cellulose nitrate filter and ABZ and RBZ concentrations were determined in a Boeco S-26 spectrophotometer at 294 and 284 nm, respectively. The inclusion complex formation constants (K_f) were calculated by Eq. 1:

$$K_f = \frac{S}{S_0(1-S)} \tag{1}$$

where S_0 is the API intrinsic solubility and S is the slope obtained by plotting the phase-solubility diagrams (37).

Preparation of Physical Mixtures and Inclusion Complexes

The complexes were prepared in 1:1 M ratio. Briefly, ABZ and RBZ were solubilized in glacial acetic acid. On the other hand, CDs were solubilized in bidistilled water. Drug and CD solutions were mixed under stirring and immediately dried in a Büchi Mini Spray Dryer B-290. The studies were performed under the following conditions: temperature 130°C, pump efficiency 15% (flow rate 5 mL/min), and aspirator set 100%. The solid product obtained was kept in an oven at 40°C for 24 h. In addition, physical mixtures were prepared in a mortar for comparison.

Apparent Solubility

The apparent solubility of ABZ and RBZ in the CD inclusion complexes and physical mixtures were determined adding an excess amount of complex (corresponding to 10 mg of API) in vials with 5 mL of bidistilled water, in an orbital shaker at 180 rpm for 72 h. Afterward, the solutions were filtered and the concentration of APIs was determined by UV spectroscopy.

Characterization of the Physical Mixtures and the Inclusion Complexes

Fourier-Transform Infrared Spectroscopy. Fourier-transform infrared spectra were obtained by an FT-IR-Prestige-21 Shimadzu (Tokyo, Japan) using the KBr disk method (2 mg sample in 100 mg KBr). Scanning range was 450 to 3900 cm^{-1} with a resolution of 1 cm^{-1}.

Differential Scanning Calorimetry. Differential scanning calorimetry (DSC) was performed on a Shimadzu TA-60 (Kyoto, Japan) calorimeter, using 5-mg samples in crimped aluminum pans. The instrument was calibrated with indium and zinc as standards. Nitrogen was used as a purge gas, and an empty aluminum pan was employed as a reference. Each sample was scanned at a rate of 5°C/min from 25 to 350°C, under N_2 atmosphere (flow rate 30 mL/min).

X-ray Diffraction. Data collection was carried out in transmission mode on an automated X'Pert Philips MPD diffractometer (Eindhoven, Netherlands). X-ray diffraction patterns were recorded using CuKα radiation ($\lambda = 1.540562$ Å), 40 kV voltage, 20 mA current, and steps of 0.02° on the interval $2\theta = 10°$–40°. Low peak broadening and background were assured by using parallel beam geometry with an X-ray lens and a graphite monochromator placed before the detector window. Data acquisition and evaluation were performed with the Stoe Visual-Xpow package, Version 2.75 (Germany).

NMR Experiments. Two-dimensional rotating-frame Overhauser effect spectroscopy (ROESY) experiments were carried to confirm complexation of ABZ and RBZ with the studied β-CDs, as well as to characterize their binding mode. The RBZ:C-β-CD complex (10 mg) was solubilized in 0.5 mL 0.1 N DCl in D_2O. ROESY measurements were performed with a Bruker Avance 300 instrument (Karlsruhe, Germany) with a 5-mm probe using the roesyph pulse sequence (Bruker) with the experimental conditions as follows: 32 scans, acquisition time 0.295 s, pulse delay 1.92 s, and 512 data points. Resonance at 4.7 ppm was used as an internal reference due to residual solvent water.

Dissolution Studies. Dissolution studies were performed in 900 mL 0.1 N HCl at 37°C, according to the US Pharmacopeia [49] by using an Apparatus 2 (SR8 8-Flask Bath, Hanson Research, Chatsworth, CA) with paddle rotating at 50 rpm. Samples of ABZ and RBZ pure drug, physical mixtures, or spray-dried complexes equivalent to 100 mg of the drug were spread on the surface of the dissolution medium and the time 0 was recorded. At appropriate time intervals, 5-mL samples were withdrawn and filtered (pore size 0.45 mm). The amount of drug released was determined by UV analysis, measuring the absorbance spectrophotometrically at 291 nm (ABZ) and 289 nm (RBZ).

In Vitro Studies

Drug Content Determination. Drug content determination has been done as follows: an accurately weighed quantity of the inclusion complexes (10.0 mg) was dissolved in 100 mL 0.1 N HCl. Drug concentration was measured spectrophotometrically. The obtained value was $15.9 \pm 0.5\%$ *w/w*.

Doses of ABZ:C-β-CD inclusion complex were calculated according to the ABZ content and corresponded to 30 mg of ABZ *per* kilogram of body weight.

Stock Solutions. Stock solutions were prepared in DMSO (37.7 mM ABZ and 35.5 mM RBZ and their inclusion complexes with C-β-CD), then were diluted in phosphate-buffered saline (pH 7.4) and finally in complete RPMI 1640 medium until reaching the desired concentration. The final concentration of DMSO did not exceed 0.1%.

Cell Proliferation Assay. Cell proliferation assay was carried out to determine the effect of the benzimidazole compounds on proliferative activity of 4T1 cell line. Briefly, 2×10^3 cells/well were seeded in 96-well plates and cultured in RPMI 1640 medium, which was supplemented with 10% fetal bovine serum and 1% antibiotic (penicillin 10 U/mL + streptomycin 10 μg/mL), at 37 °C in a 5% CO_2 atmosphere for 8 h to allow cell attachment. Then, the medium was replaced by free-drug or complex-drug solution.

After 48 h of incubation, WST-1 reagent was added and the absorbance was read on a Rayto RT-2100C microplate reader (Shenzhen, P. R. China).

Half maximal inhibitory concentration (IC50) values were obtained from the absorbance curves as function of the API concentration by using GraphPad Prism 7 (GraphPad Software, La Jolla, CA, USA).

In Vivo Studies

Six to 8-week-old BALB/c mice were obtained from ICiVet-Litoral (Esperanza, Santa Fe, Argentina). All experiments were performed in accordance with the Canadian Council on Animal Care guidelines [50]. Animals were fed with commercial chow and water *ad libitum* and maintained in a 12-h light/dark cycle.

In order to assess primary breast cancer cell growth, 5×10^4 4T1 cells were resuspended in PBS and injected (100 μL) orthotopically into the right mammary gland of the recipient mouse. When tumors reached ~ 150 mm^3, animals ($n = 5$–8/group) were randomly distributed in three groups as follows: control (no treatment), ABZ, and ABZ:C-β-CD complex.

Table I. Values of Equilibrium Constants of the Complexes (K_f, M^{-1}). R^2 Values Obtained from the Linear Fit Are Indicated in Parentheses [37]

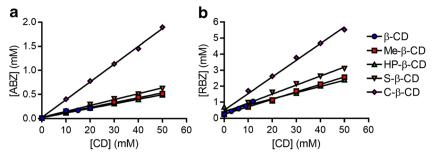|	ABZ	RBZ
β-CD	74 (0.722)	212 (0.998)
Me-β-CD	337 (0.995)	197 (0.999)
HP-β-CD	313 (0.996)	177 (0.999)
S-β-CD	515 (0.995)	124 (0.984)
C-β-CD	1037 (0.998)	287 (0.993)

Fig. 1. Phase solubility diagram. Concentration of ABZ and RBZ against increasing concentrations of CDs

These last two groups were treated with 30-mg ABZ/kg oral doses, three times weekly for 53 days. Tumor growth was analyzed by measuring tumor length (a) and width (b) with a caliper, and by calculating tumor volume (V) with Eq. 2 [51]:

$$V = 0.4ab^2 \tag{2}$$

Data were fit to an exponential growth curve and a two-tailed Student's t test was performed in GraphPad Prism software 7 (GraphPad Software, La Jolla, CA, USA).

When tumors reached the largest ethically permitted volume, animals were euthanized and their lungs excised and fixed, and the number and size of metastatic foci determined macroscopically. Absence of symptoms of toxicity in the animals was verified on a daily basis.

RESULTS AND DISCUSSION

Characterization of the Physical Mixtures and Inclusion Complexes

Fourier-transform infrared spectroscopy, differential scanning calorimetry, and X-ray diffraction studies have been done to analyze the solid state of ABZ and RBZ in physical mixtures and in the CD inclusion complexes (data not shown).

Those results suggest that ABZ and RBZ are in an amorphous state after the complex formation process [37, 52].

Phase Solubility Diagrams

CDs could enhance apparent water solubility by forming dynamic, water-soluble inclusion complexes [42]. This interaction is an equilibrium governed by an equilibrium constant, K_f. A_L-type profiles (linear relationship) were obtained by plotting ABZ or RBZ concentration and increasing concentration of CDs. A-type profiles represent the formation of water-soluble CD complexes in 1:1 M ratio [42].

K_f calculated values are shown in Table I and Fig. 1 shows the A-type profiles.

ABZ and RBZ presented the highest K_f values using C-β-CD as an excipient. Solubility improvement could be attributed to the stabilization of the complex by electrostatic interactions between the positive charge of the API and the negative charge of the C-β-CD.
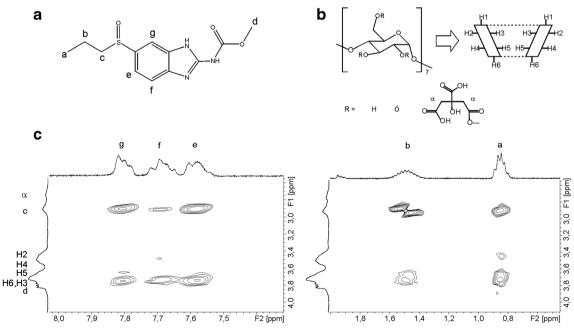

Fig. 2. ROESY spectrum. **a** RBZ proton labelling. **b** C-β-CD proton labelling. **c** Plot of two-dimensional ROESY spectrum of RBZ in the presence of C-β-CD

Table II. Apparent Solubility Values of Complexes and Physical Mixtures. The Values Are Expressed as Mean (mg/mL) ± Standard Deviation [37]

	ABZ	RBZ
API	0.0013 ± 0.0007	0.06 ± 0.02
β-CD complex	0.024 ± 0.001	2.331 ± 0.004
β-CD physical mixture	0.013 ± 0.002	0.28 ± 0.01
Me-β-CD complex	0.069 ± 0.002	4.3 ± 0.1
Me-β-CD physical mixture	0.016 ± 0.001	0.9 ± 0.4
HP-β-CD complex	0.048 ± 0.001	3.2 ± 0.4
HP-β-CD physical mixture	0.011 ± 0.004	1.00 ± 0.05
S-β-CD complex	0.143 ± 0.003	4.7 ± 0.7
S-β-CD physical mixture	0.016 ± 0.002	1.11 ± 0.05
C-β-CD complex	0.799 ± 0.009	6.7 ± 0.7
C-β-CD physical mixture	0.172 ± 0.004	1.9 ± 0.1

Differences in K_f values between both APIs in the presence of C-β-CD may be due to a lower hydrophobicity of RBZ in comparison with ABZ due to the presence of the sulfoxide group in the molecule of RBZ.

NMR Experiments

The characterization of the CD derivative and the inclusion complex is extremely important to understand the host-guest molecule interaction. Different NMR spectroscopy analyses (^{1}H-^{13}C heteronuclear single-quantum correlation, HSQC, heteronuclear multiple bond correlation, HMBC, and rotating-frame overhauser effect spectroscopy, ROESY) were used to study the structural characteristics of supramolecular aggregates. ROESY NMR experiment provides information for investigating inter- and intra-molecular interactions and it is relevant in order to determine the possible inclusion mode of complexes. In this technique, the observation of ROESY cross-peaks indicates that the distance between the involved hydrogen nuclei is below 0.4 nm.

ROESY spectrum of the system ABZ:C-β-CD was previously described (Garcia *et al.* 2014) [37].

The proton labels of RBZ and C-β-CD and the partial ROESY spectrum of the system RBZ:C-β-CD are shown in Fig. 2. In this figure, cross-peaks between the internal C-β-CD protons and "e" ($\delta = 7.57$ ppm), "f" ($\delta = 7.68$ ppm), and "g" ($\delta = 7.80$ ppm) protons that pertain to aromatic ring of RBZ could be observed. In addition, intermolecular cross-peaks were observed between the "a" ($\delta = 0.85$ ppm) and "b" ($\delta = 1.50$ ppm) protons and the internal protons of C-β-CD. These results indicated that the non-polar portion of the guest structure could be included in the cavity of C-β-CD. Similar interactions were observed for ABZ:C-β-CD, as it was described in Garcia *et al.* (2013).

Apparent Solubility and Dissolution Profiles

Tables II and III show the apparent solubility and drug release values of API formulations (inclusion complexes and physical mixtures). As might be expected, solubility and dissolution rate increased in the presence of CDs observing better results for inclusion complexes than physical mixtures. The most important increase in solubility was observed employing the C-β-CD inclusion complexes. ABZ solubility increased 615 times compared to the ABZ as a pure drug, while RBZ, 112 times. Apparent solubility values for the C-β-CD complexes are according to the K_f values.

Drug release results showed a clear improvement in the dissolution rate of the CD inclusion complexes, suggesting a benefit for potential oral dosage forms.
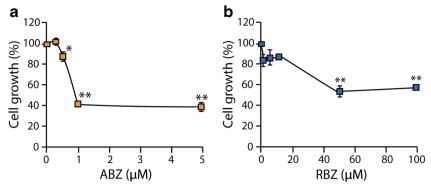
Effect of ABZ and RBZ and Their Cyclodextrin Inclusion Complexes on Cell Proliferation and Their Cyclodextrin Inclusion Complexes on Cell Proliferation

Both benzimidazole compounds presented anti-proliferative activity on 4T1 cell line. The decrease in cell growth was dose dependent, but a saturation effect was reached as shown in Fig. 3. While ABZ concentrations higher

Table III. *In Vitro* Dissolution Data of Inclusion Complexes and Physical Mixtures. Drug Released (%) at 10, 30, and 60 min (Q_{10}, Q_{30}, and Q_{60}) ± Standard Deviation

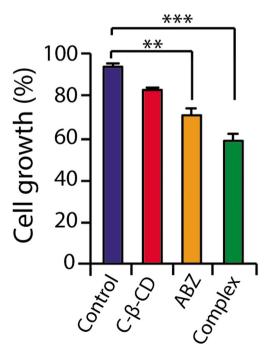| Sample	ABZ			RBZ	
	Q_{10} (%)	Q_{30} (%)	Q_{60} (%)	Q_{10} (%)	Q_{30} (%)
API	2.0 ± 1.0	3.8 ± 2.1	6.1 ± 2.9	68.5 ± 0.4	100.5 ± 0.7
β-CD complex	23.7 ± 2.2	34.5 ± 1.9	46.6 ± 1.4	102.8 ± 0.5	–
β-CD physical mixture	3.2 ± 0.6	7.7 ± 0.1	12.6 ± 0.2	99.6 ± 1.1	–
Me-β-CD complex	101.1 ± 2.2	99.0 ± 2.1	94.8 ± 1.3	101.6 ± 3.3	–
Me-β-CD physical mixture	53.2 ± 0.7	62.9 ± 1.1	68.3 ± 1.4	104.2 ± 2.7	–
HP-β-CD complex	39.8 ± 2.3	54.8 ± 2.0	65.6 ± 1.2	103.1 ± 2.1	–
HP-β-CD physical mixture	13.0 ± 1.9	22.5 ± 0.9	31.3 ± 1.1	102.5 ± 1.2	–
S-β-CD complex	77.1 ± 2.5	91.8 ± 0.4	95.5 ± 1.9	103.0 ± 3.4	–
S-β-CD physical mixture	10.7 ± 2.4	25.2 ± 2.2	44.3 ± 3.2	100.5 ± 2.3	–
C-β-CD complex	92.7 ± 2.2	97.5 ± 2.1	96.8 ± 1.3	98.5 ± 0.3	–
C-β-CD physical mixture	34.3 ± 2.4	49.0 ± 2.2	57.0 ± 3.2	104.0 ± 0.4	–

– Totally dissolved

Fig. 3. Cells were cultured in the presence of increasing doses of ABZ or RBZ during 48 h. The number of metabolically active cells was estimated by tetrazolium salts reduction method ($n = 3$; *$p < 0.05$, **$p < 0.01$)

than 0.5 μM significantly decreased cell growth, higher concentrations of RBZ were required to achieve the same effect. For this reason, we decided to focus our studies on the antitumor effect of ABZ.

A recent study in a breast cancer model (MCF-7 cells) showed that ABZ inhibited cell viability [1]. Nevertheless, it is worthwhile to note that we obtained the same results in a more aggressive model. Among breast cancer subtypes, triple-negative breast cancer exhibits distinct characteristics, is particularly aggressive and frequently recurrent, and becomes metastatic [3]. These subtypes of tumors account for 15% of all breast cancer types with higher percentages in premenopausal African-American and Hispanic women, and it is associated with very poor prognosis and limited treatment option availability [51]. As shown in Fig. 4, the

ABZ:C-β-CD complex decreased significantly 4T1 cell growth when compared to the untreated control. Noteworthy, differences were not statistically significant between cells exposed to CDs and control cells.

The IC50 value obtained for ABZ was 0.56 ± 0.02 μM while for the ABZ:C-β-CD complex was 0.41 ± 0.30 μM. Although ABZ:C-β-CD complex showed lower values of IC50 than ABZ, no statistically significant differences were observed.

In Vivo Studies

The effect of treatment with ABZ and ABZ:C-β-CD complex on 4T1 cells in BALB/c mice was analyzed (Fig. 5). Mice treated with the ABZ:C-β-CD complex developed tumors which showed significantly slower growth kinetics compared with the other groups. After 53 days of inoculation, significant differences in tumor volume were observed between complex and the other treatments ($p < 0.01$). These results show the potentiality of the ABZ complex to reduce significantly the volume of tumors. The examination of animals, at the end of the assay, indicated no differences in the number of lung metastasis (data not shown).
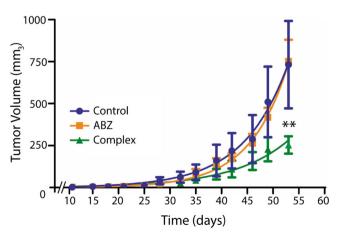

Fig. 4. Cells were cultured in the presence of the ABZ, C-β-CD, and ABZ:C-β-CD complex (0.5 μM) during 48 h. The number of metabolically active cells was estimated by tetrazolium salts reduction method ($n = 3$; **$p < 0.01$, ***$p < 0.001$)

Fig. 5. Immunocompetent mice were orthotopically challenged with 4T1 cells. Tumor size was measured biweekly with a caliper (**$p < 0.01$)

CONCLUSIONS

Inclusion complexes of ABZ and RBZ were prepared with β-CD and its derivatives. The apparent solubility of the APIs was highest when C-β-CD derivative was used as carrier. This increase in solubility was higher for ABZ, indicating the formation of a more stable complex than with RBZ. Additionally, ABZ showed *in vitro* anti-proliferative activity at lower doses than RBZ on 4T1 cell line. Furthermore, *in vivo* studies showed that ABZ:C-β-CD complex allowed reducing the tumor growth kinetics on BALB/c mice with no signs of toxicity. These findings can lead to an effective therapy against triple-negative breast cancer by combining of ABZ:C-β-CD complex with other antitumor drugs.

COMPLIANCE WITH ETHICAL STANDARDS

All experiments were performed in accordance with the Canadian Council on Animal Care guidelines.

Animal Studies All institutional and national guidelines for the care and use of laboratory animals were followed. This study was authorized by the Ethics Committee for Animal Use (registration number 1659/2016).

REFERENCES

1. Castro LSEPW, Kviecinski MR, Ourique F, Parisotto EB, Grinevicius VMAS, Correia JFG, et al. Albendazole as a promising molecule for tumor control. Redox Biol. 2016;10:90–9.
2. Gupta SC, Sung B, Prasad S, Webb LJ, Aggarwal BB. Cancer drug discovery by repurposing: teaching new tricks to old dogs. Trends Pharmacol Sci. 2013;34(9):508–17.
3. Bhatnagar S, Kumari P, Pattarabhiran SP, Venuganti VVK. Zein microneedles for localized delivery of chemotherapeutic agents to treat breast cancer: drug loading, release behavior, and skin permeation studies. AAPS PharmSciTech. 2018;19(4):1818–26.
4. Kassem MA, Megahed MA, Abu Elyazid SK, Abd-Allah FI, Abdelghany TM, Al-Abd AM, et al. Enhancing the therapeutic efficacy of tamoxifen citrate loaded span-based nano-vesicles on human breast adenocarcinoma cells. AAPS PharmSciTech. 2018;19(4):1529–43.
5. Boguski MS, Mandl KD, Sukhatme VP. Repurposing with a difference. Science. 2009;324(5933):1394–5.
6. Dudley J, Berliocchi L. Drug repositioning: approaches and applications for neurotherapeutics. Boca Raton: CRC press; 2017.
7. Yoshida GJ. Therapeutic strategies of drug repositioning targeting autophagy to induce cancer cell death: from pathophysiology to treatment. J Hematol Oncol. 2017;10(1):67.
8. Luther MA. Systems pharmacology and drug repositioning- an integrated approach to metabolic diseases. J Transl Med. 2012;10(2):A18.
9. Wu C, Gudivada RC, Aronow BJ, Jegga AG. Computational drug repositioning through heterogeneous network clustering. BMC Syst Biol. 2013;7(5):S6.
10. Andre N, Banavali S, Snihur Y, Pasquier E. Has the time come for metronomics in low-income and middle-income countries? Lancet Oncol. 2013;14(6):e239–48.
11. Liang X-J, Chen C, Zhao Y, Wang PC. Circumventing tumor resistance to chemotherapy by nanotechnology. Multi-Drug Resistance in Cancer. Berlin: Springer; 2010. p. 467–88.
12. Tobinick EL. The value of drug repositioning in the current pharmaceutical market. Drug News Perspect. 2009;22(2):119–25.
13. Bisgin H, Liu Z, Kelly R, Fang H, Xu X, Tong W. Investigating drug repositioning opportunities in FDA drug labels through topic modeling. BMC Bioinformatics. 2012;13(15):S6.
14. Ferrero E, Agarwal P. Connecting genetics and gene expression data for target prioritisation and drug repositioning. BioData Mining. 2018;11(1):7.
15. Napolitano F, Zhao Y, Moreira VM, Tagliaferri R, Kere J, D'Amato M, et al. Drug repositioning: a machine-learning approach through data integration. J Cheminform. 2013;5(1):30.
16. Nygren P, Fryknäs M, Ågerup B, Larsson R. Repositioning of the anthelmintic drug mebendazole for the treatment for colon cancer. J Cancer Res Clin Oncol. 2013;139(12):2133–40.
17. Bongioanni A, Araujo BS, de Oliveira YS, Longhi MR, Ayala A, Garnero C. Improving properties of albendazole desmotropes by supramolecular systems with maltodextrin and glutamic acid. AAPS PharmSciTech. 2018;19(3):1468–76. https://doi.org/10.1208/s12249-018-0952-0.
18. Priotti J, Leonardi D, Pico G, Lamas MC. Application of fluorescence emission for characterization of albendazole and ricobendazole micellar systems: elucidation of the molecular mechanism of drug solubilization process. AAPS PharmSciTech. 2018;19(3):1152–9. https://doi.org/10.1208/s12249-017-0927-6.
19. Riviere JE, Papich MG. Veterinary pharmacology and therapeutics. Hoboken: Wiley; 2009.
20. Priotti J, Codina AV, Leonardi D, Vasconi MD, Hinrichsen LI, Lamas MC. Albendazole microcrystal formulations based on chitosan and cellulose derivatives: physicochemical characterization and in vitro parasiticidal activity in Trichinella spiralis adult worms. AAPS PharmSciTech. 2017;18(4):947–56.
21. García A, Barrera MG, Piccirilli G, Vasconi MD, Di Masso RJ, Leonardi D, et al. Novel albendazole formulations given during the intestinal phase of Trichinella spiralis infection reduce effectively parasitic muscle burden in mice. Parasitol Int. 2013;62(6):568–70. https://doi.org/10.1016/j.parint.2013.08.009.
22. Walter HS, Ahmed S. Targeted therapies in cancer. Surgery (Oxford). 2018;36(3):122–7.
23. Chu SWL, Badar S, Morris DL, Pourgholami MH. Potent inhibition of tubulin polymerisation and proliferation of paclitaxel-resistant 1A9PTX22 human ovarian cancer cells by albendazole. Anticancer Res. 2009;29(10):3791–6.
24. Noorani L, Stenzel M, Liang R, Pourgholami MH, Morris DL. Albumin nanoparticles increase the anticancer efficacy of albendazole in ovarian cancer xenograft model. J Nanobiotech. 2015;13(1):25.
25. Ehteda A, Galettis P, Chu SW, Pillai K, Morris DL. Complexation of albendazole with hydroxypropyl-beta-cyclodextrin significantly improves its pharmacokinetic profile, cell cytotoxicity and antitumor efficacy in nude mice. Anticancer Res. 2012;32(9):3659–66.
26. Ehteda A, Galettis P, Pillai K, Morris DL. Combination of albendazole and 2-methoxyestradiol significantly improves the survival of HCT-116 tumor-bearing nude mice. BMC Cancer. 2013;13(1):86.
27. Kutlehria S, Behl G, Patel K, Doddapaneni R, Vhora I, Chowdhury N, et al. Cholecalciferol-PEG conjugate based nanomicelles of doxorubicin for treatment of triple-negative breast cancer. AAPS PharmSciTech. 2018;19(2):792–802.
28. Sorlie T, Tibshirani R, Parker J, Hastie T, Marron JS, Nobel A, et al. Repeated observation of breast tumor subtypes in independent gene expression data sets. Proc Natl Acad Sci U S A. 2003;100(14):8418–23.

29. Haser A, Zhang F. New strategies for improving the development and performance of amorphous solid dispersions. AAPS PharmSciTech. 2018;19(3):978–90.

30. Zhang Y, Huang Y, Li S. Polymeric micelles: nanocarriers for cancer-targeted drug delivery. AAPS PharmSciTech. 2014;15(4):862–71.

31. Priotti J, Leonardi D, Pico G, Lamas MC. Application of fluorescence emission for characterization of albendazole and ricobendazole micellar systems: elucidation of the molecular mechanism of drug solubilization process. AAPS PharmSciTech. 2017:1–8.

32. Brough C, Williams Iii RO. Amorphous solid dispersions and nano-crystal technologies for poorly water-soluble drug delivery. Int J Pharm. 2013;453(1):157–66.

33. Zhang Y, Hu X, Liu X, Dandan Y, Di D, Yin T, et al. Dry state microcrystals stabilized by an HPMC film to improve the bioavailability of andrographolide. Int J Pharm. 2015;493(1–2):214–23.

34. Bavishi DD, Borkhataria CH. Spring and parachute: how cocrystals enhance solubility. Prog Cryst Growth Charact Mater. 2016;62(3):1–8.

35. Real D, Leonardi D, Williams RO III, Repka MA, Salomon CJ. Solving the delivery problems of triclabendazole using cyclodextrins. AAPS PharmSciTech. 2018;19:2311–21.

36. García A, Leonardi D, Lamas MC. Promising applications in drug delivery systems of a novel β-cyclodextrin derivative obtained by green synthesis. Bioorg Med Chem Lett. 2016;26(2):602–8.

37. García A, Leonardi D, Salazar MO, Lamas MC. Modified β-cyclodextrin inclusion complex to improve the physicochemical properties of albendazole. Complete in vitro evaluation and characterization. PLoS One. 2014;9(2):e88234.

38. Ferreira MJG, García A, Leonardi D, Salomon CJ, Lamas MC, Nunes TG. 13C and 15N solid-state NMR studies on albendazole and cyclodextrin albendazole complexes. Carbohydr Polym. 2015;123:130–5.

39. García A, Leonardi D, Vasconi MD, Hinrichsen LI, Lamas MC. Characterization of albendazole-randomly methylated-β-cyclodextrin inclusion complex and in vivo evaluation of its antihelmitic activity in a murine model of trichinellosis. PLoS One. 2014;9(11):e113296.

40. Duchêne D, Bochot A. Thirty years with cyclodextrins. Int J Pharm. 2016;514(1):58–72.

41. Conceição J, Adeoye O, Cabral-Marques HM, Lobo JMS. Cyclodextrins as excipients in tablet formulations. Drug Discov Today. 2018;23:1274–84.

42. Kurkov SV, Loftsson T. Cyclodextrins. Int J Pharm. 2013;453(1):167–80.

43. Szente L, Szejtli J. Highly soluble cyclodextrin derivatives: chemistry, properties, and trends in development. Adv Drug Deliv Rev. 1999;36(1):17–28.

44. Leonardi D, Bombardiere ME, Salomon CJ. Effects of benznidazole:cyclodextrin complexes on the drug bioavailability upon oral administration to rats. Int J Biol Macromol. 2013;62:543–8.

45. Codina AV, García A, Leonardi D, Vasconi MD, Di Masso RJ, Lamas MC, et al. Efficacy of albendazole:β-cyclodextrin citrate in the parenteral stage of Trichinella spiralis infection. Int J Biol Macromol. 2015;77:203–6.

46. Mura P. Analytical techniques for characterization of cyclodextrin complexes in the solid state: a review. J Pharm Biomed Anal. 2015;113:226–38.

47. Hay WT, Behle RW, Fanta GF, Felker FC, Peterson SC, Selling GW. Effect of spray drying on the properties of amylose-hexadecylammonium chloride inclusion complexes. Carbohyd Polym. 2017;157:1050–6.

48. Medarević D, Kachrimanis K, Djurić Z, Ibrić S. Influence of hydrophilic polymers on the complexation of carbamazepine with hydroxypropyl-β-cyclodextrin. Eur J Pharm Sci. 2015;78:273–85.

49. United States Pharmacopeial Convention. The United States Pharmacopeia. Rockville, Maryland 2012;35th ed.

50. Baar M, Dale J, Griffin G. Chapter 3 - Canada's oversight of animal ethics and care in science. In: Guillén J, editor. Laboratory Animals. 2nd ed. Cambridge: Academic Press; 2018. p. 69–90.

51. Rico M, Baglioni M, Bondarenko M, Laluce NC, Rozados V, Nicolas A, et al. Metformin and propranolol combination prevents cancer progression and metastasis in different breast cancer models. Oncotarget. 2017;8(2):2874–89.

52. Wu Z, Razzak M, Tucker IG, Medlicott NJ. Physicochemical characterization of ricobendazole: I. solubility, lipophilicity, and ionization characteristics. J Pharm Sci. 2005;94(5):983–93.